山西大学学报(自然科学版)44(2):287－293,2021
Journal of Shanxi University(Nat. Sci. Ed.)

DOI:10.13451/j.sxu.ns.2020113

瞬烯类似物$C_9H_9^+$、C_9BH_9和C_8NH_9中的流变键

高彩月,马媛媛,闫苗,李思殿*
(山西大学 分子科学研究所,山西 太原 030006)

摘　要:结构流变是化学中熟知的现象,但人们对分子流变过程的成键本质尚认识不足。文章提出化学中的“流变键”(Fluxional Bonds,FBs)概念,并将其成功应用于平面、笼状和管状硼团簇及瞬烯分子$C_{10}H_{10}$,揭示了化学结构流变的成键本质。与传统的由于化学键的伸缩、弯曲和摇摆等产生的Berry准旋转不同,流变键在一定条件下可以不断地破裂和生成,是分子结构流变的驱动力。文章继续研究瞬烯类似物$C_9H_9^+$、C_9BH_9和C_8NH_9中的流变键,在分子轨道水平上揭示其流变机理。详尽的轨道和成键分析表明,这些模型化合物中存在与瞬烯相似的流变键。在从基态(GS)到过渡态(TS)的流变过程中,$C_9H_9^+$主要涉及两个流变σ键的变化(GS(1 2c-2e σ + 1 3c-2e σ) → TS(2 2c-2e σ) → GS′(1 2c-2e σ + 1 3c-2e σ)),而C_9BH_9和C_8NH_9则是两个π键(GS(2 2c-2e π) → TS(2 3c-2e π) → GS′(2 2c-2e π))和一个σ键(GS(1 2c-2e σ) → TS(1 4c-2e σ) → GS′(1 2c-2e σ))协同流变的结果。流变键采用联系、运动和变化的观点分析化学成键,是对化学中传统定域和离域成键概念的拓展,预计在催化、纳米材料和分子马达研究中具有重要意义。

关键词:瞬烯类似物;第一性原理计算;结构;成键;流变键
中图分类号:O641.4　　**文献标志码**:A　　**文章编号**:0253-2395(2021)02-0287-07

Fluxional bonds in analogs of bullvalene $C_9H_9^+$, C_9BH_9 and C_8NH_9

GAO Caiyue, MA Yuanyuan, YAN Miao, LI Sidian*
(*Institute of Molecular Science, Shanxi University, Taiyuan* 030006, *China*)

Abstract:Chemical bond is the most important concept in chemistry. This paper proposed the concept of fluxional bonds which form and break constantly under certain conditions and applied it successfully to various boron clusters and bullvalene $C_{10}H_{10}$, unveiling the fluxional bonding nature of these important species. We continue in this work to explore the fluxional bonds in analogs of bullvalene, $C_9H_9^+$, C_9BH_9 and C_8NH_9, to reveal the bonding fluctuation mechanisms of these interesting species at molecular orbital level. The detailed orbital and bonding analyses indicate that the fluxional bonds of these model compounds exhibit obvious similarity with that of bullvalene. The fluxional process of $C_9H_9^+$ mainly involves two fluxional σ-bonds from the ground state (GS) to transition state (TS) (GS(1 2c-2e σ + 1 3c-2e σ) → TS(2 2c-2e σ) → GS′(1 2c-2e σ + 1 3c-2e σ)), while the fluctuations of both C_9BH_9 and C_8NH_9 involve two fluxional π-bonds (GS(2 2c-2e π) → TS(2 3c-2e π) →GS′(2 2c-2e π)) and one fluxional σ-bond (GS(1 2c-2e σ) → TS(1 4c-2e σ) → GS′(1 2c-2e σ)) in concerted mechanisms.

Key words: analogs of bullvalene; first-principles calculation; structures; bonding; fluxional bonds

---

收稿日期:2020-10-01;**接受日期**:2020-11-28
基金项目:重点国际(地区)合作研究项目(21720102006)

作者简介:高彩月(1997-),女,山西交口人,博士研究生,主要研究方向为纳米团簇结构与性质研究。E-mail:gaocaiyue@sxu.edu.cn

* **通信作者**:李思殿(LI Sidian),E-mail:lisidian@sxu.edu.cn

引文格式:高彩月,马媛媛,闫苗,等. 瞬烯类似物$C_9H_9^+$、C_9BH_9和C_8NH_9中的流变键[J]. 山西大学学报(自然科学版),2021,44(2):287-293. DOI:10.13451/j.sxu.ns.2020113

1　Introduction

Various molecules are known in chemistry to exhibit structural fluxionalities under certain conditions. Typical fluxional molecules include iron pentacarbonyl $Fe(CO)_5$, phosphorus pentafluoride PF_5, dimethylformamide $(CH_3)_2NC(O)H$, and protonated methane CH_5^+ which undergo Berry pseudo-rotations through the bending, swaying, or stretching of localized two-center-two-electron (2c-2e) σ bonds[1-6]. No chemical bonds are formed or broken in the fluxional processes of these molecules. Our group recently proposed the concept of fluxional bonds (FBs) in planar B_{19}^-, tubular $Ta@B_{20}^-$, and cage-like B_{39}^-, as an extension of the classical localized and delocalized bonds known in chemistry[7]. FBs in these species form and break constantly under certain conditions at finite temperatures. We also reported multi-center FBs in half-sandwich MB_{18}^- (M = K, Rb and Cs) [8] and NiB_{11}^-[9], planar or quasi-planar C_{2v} B_{11}^- ($B_2@B_9^-$)[10], C_{2v} B_{13}^+ ($B_3@B_{10}^+$)[11-12], and C_{2v} B_{15}^+ ($B_4@B_{11}^+$)[13-14], and tubular B_3-[Ta@B_{18}], B_4-[Ta@B_{18}]$^+$, and $La_2[B_2@B_{18}]$[15-16]. Typical π-FBs and σ-FBs were very recently observed in the well-known fluxional molecule bullvalene ($C_{10}H_{10}$) and its analogs C_8H_8, C_9H_{10} and C_8BH_9 in rapid Cope rearrangements[17], opening the door to explore novel FBs in both stable organic molecules and important catalysis processes.

Based on extensive first-principles theory calculations and detailed bonding analyses, we report herein the existence of multi-center FBs in more bullvalene analogs including the cage-like $C_9H_9^+$, C_9BH_9 and C_8NH_9. Two fluxional σ-bonds were revealed in the fluxional process of $C_9H_9^+$, while two fluxional π-bonds and one fluxional σ-bond were identified in concerted mechanisms in both C_9BH_9 and C_8NH_9. The activation energies between the ground states and transition states and the corresponding reaction rate constants k^{TST} are predicted to facilitate future experiments.

2　Theoretical procedure and computational method

The ground state (GS) and transition state (TS) of all molecules were optimized at the DFT-PBE0 [18-20] level with the basis sets of 6-311+G(d)[21]. Frequency checks were performed to ensure that all optimized structures are true GSs or TSs. Intrinsic reaction coordinate (IRC) [22-23] path analyses were also performed to confirm the TS structures. All the PBE0 calculations in this work were performed using the Gaussian 09 package[24]. The activation energies in the fluxional processes were further refined at the more accurate CCSD(T)/6-311G(d) level [25-27] at PBE0 geometries using the Molpro program [28]. Detailed bonding analyses were performed on the GS, TS, and GS′ of the concerned species (GS′ represents the second ground state in the GS→TS→GS′ fluctuation process. It may be the same as the GS or it may be an intermediate state in the reaction path) using the adaptive natural density partitioning (AdNDP) program[29-30]. The reaction rate constant k is calculated based on the transition-state theory (TST) [31] using the following equation: [32]

$$k^{\mathrm{TST}}=\kappa\frac{k_B T}{h}e^{-\Delta G^{\neq}/(RT)}$$

where, κ, k_B, T, h, $\Delta G^{\neq}$, and R are the transmission coefficient, Boltzmann constant, temperature, Planck constant, standard activation free energy, and molar gas constant, respectively. The transmission coefficient κ can be valued by the Wigner tunneling correction[33], $\kappa = 1 + (1/24)\,[h\mathrm{Im}(v^{\neq})/k_B T]^2$, where $\mathrm{Im}(v^{\neq})$ is the imaginary frequency of the transition state. The calculated results are summarized in Table 1 to facilitate future experimental confirmations of these fluxional species.

3　Results and discussion

3.1　Structures and stabilities

The closed-shell C_{3v} GS (1), C_{2v} TS (2) and C_{3v} GS' (3) of $C_9H_9^+$ in Fig. 1 are constructed by removing one CH group from the experimentally known C_{3v} GS, C_{2v} TS, and C_{3v} GS′ of $C_{10}H_{10}$[17], respectively. Similarly, C_{3v} GS (4), C_s TS (5) and C_s GS' (6) of C_9BH_9 can be obtained by substituting one CH group in $C_{10}H_{10}$ with a trivalent B atom. C_s GS (7), C_s TS (8), and C_s GS' (9) of C_8NH_9 are achieved by substituting one C atom in $C_9H_9^+$ with a trivalent N (Fig. 1). There exists a three-center bonding interaction between C3, C4 and C5 in the C_{3v} GS (1) which is the true GS of the monocation with no imaginary vibrational frequency. The corresponding degenerate C_{3v} GS' (3) can be obtained by turning the C_{3v} GS (1) structure up-down. The C_{2v} $C_9H_9^+$ (2) as the transition state between C_{3v} GS (1) and C_{3v} GS′ (3) has one imaginary frequency at −544. 33 cm^{-1}. As can be seen from the bond lengths indicated in Fig. 1, the distance between C3—C4 at the bottom with r_{C3-C4} = 1. 81 Å in the GS has been shortened to r_{C3-C4} = 1. 57 Å in the TS, while the C1—C2 single bond on the top with r_{C1-C2} = 1. 51 Å in the GS has been elongated to $r_{C1\text{-}C2}$ = 1. 57 Å in the TS. That is, a C3—C4 single σ bond is formed in the TS while the C1—C2 σ bond in the GS is to be broken. From the TS C_{2v} $C_9H_9^+$ (2) to the GS' C_{3v} $C_9H_9^+$ (3), the opposite process occurs. In the fluxional process of GS→TS→GS', the upward and downward sways of C5 induce the structural fluctuation of the monocation. The calculated activation energy of ΔE_a = 22. 87 kcal·mol^{-1} at CCSD(T) from the GS to the TS of $C_9H_9^+$ approximately doubles the corresponding value of ΔE_a = 12. 9 kcal·mol^{-1} calculated for bullvalene $C_{10}H_{10}$ at the same level of theory[17].

The C_{3v} GS (4) of C_9BH_9 contains three equivalent C—C σ bonds on the top and three equivalent C=C double bonds on the waist. Its transition state C_s C_9BH_9 (5) has one imaginary frequency at −254. 58 cm^{-1}. The C1—C2 distance r_{C1-C2} = 1. 53 Å in C_{3v} C_9BH_9 (4) has been elongated to r_{C1-C2} = 2. 15 Å in C_s C_9BH_9 (5), while

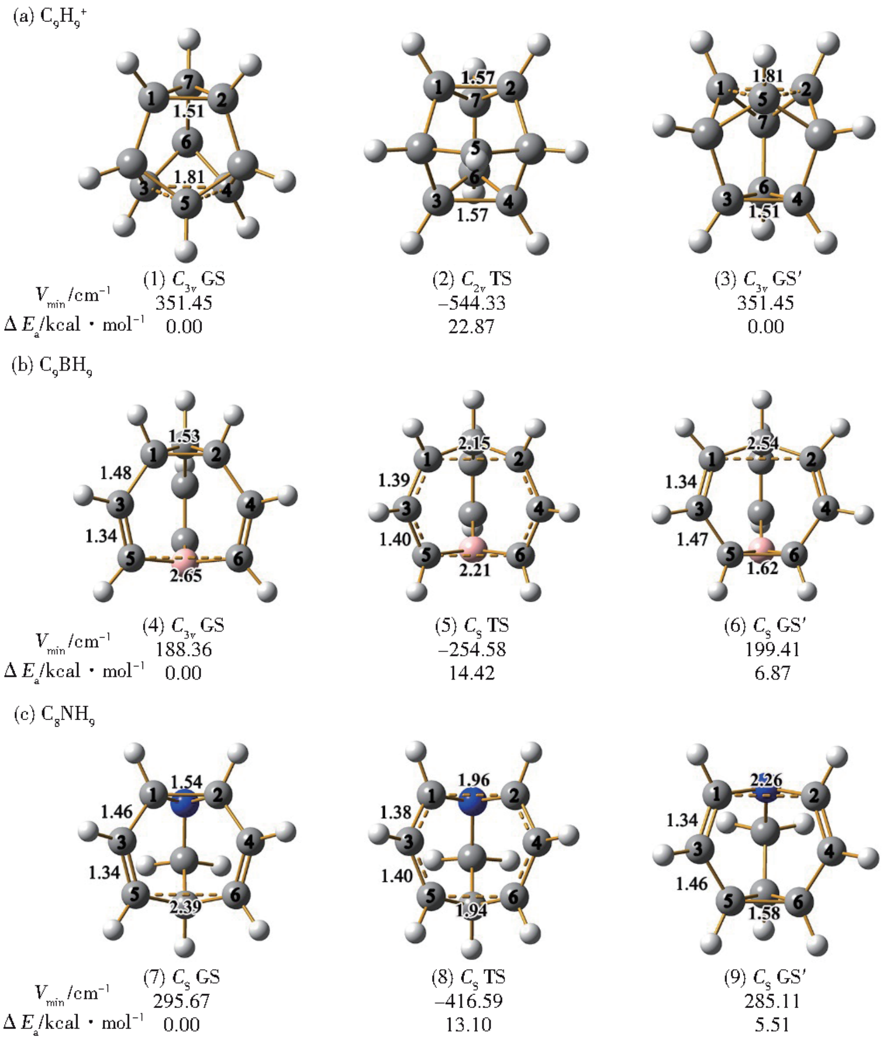

Fig. 1 Optimized structures of the ground state (GS/GS') and transition state (TS) of (a) $C_9H_9^+$, (b) C_9BH_9 and (c) C_8NH_9, with the lowest vibrational frequencies v_{min} at PBE0 level and relative energies ΔE_a at the single-point CCSD(T)//PBE0/6-311+G(d) indicated. The bond lengths are labelled in Å

C5—C6 distance $r_{c5\text{-}c6}$ = 2.65 Å in the GS has been simultaneously shortened to $r_{c5\text{-}c6}$ = 2.21 Å in the TS. The calculated C1—C3/C2—C4 (1.39 Å) and C3—C5/C4—C6 (1.40 Å) distances in the C_s TS have practically the same bond lengths. This structural fluctuation indicates the transfer of one 2c-2e σ bond on C1—C2 in the GS into one 4c-2e σ bond on C1—C2 and C5—C6 in the TS and two π bonds from two 2c-2e π bonds over C3—C5/C4—C6 in the GS to two 3c-2e π bonds over C1⋯C3⋯C5/C2⋯C4⋯C6 in the TS. The intermediate C_s GS′ (6) lies 6.87 kcal·mol^{-1} higher than the C_{3v} GS (4) in energy. It contains a newly formed C5—C6 σ bond at the bottom, with the C1—C2 interaction on the top broken.

As shown in Fig. 1, C_8NH_9 possesses similar cage-like GS, TS, and GS′ structures with C_9BH_9, with C_s C_8NH_9 (7) being 13.10 and 5.51 kcal·mol^{-1} more stable than C_s C_8NH_9 (8) and C_s C_8NH_9 (9), respectively. The calculated activation energies of C_9BH_9 and C_8NH_9 are 14.42 and 13.10 kcal·mol^{-1} from their GSs to TSs at CCSD(T) level, respectively, close to the energy barrier of 12.90 kcal·mol^{-1} calculated at the same level for $C_{10}H_{10}$[17]. The predicted rate constants k^{TST} of $C_9H_9^+$, C_9BH_9 and C_8NH_9 from their GSs to TSs and from TSs to the GSs' at 298 K in Table 1 clearly indicates that C_9BH_9 and C_8NH_9 fluctuate much more quickly than $C_9H_9^+$ due to the huge differences in their activation free energies $\Delta G^{\neq}$. It is also noticed that both the intermediate states C_s C_9BH_9 (6) and C_s C_8NH_9 (9) with higher rate constants k^{TST} are short-lived species compared to their ground states C_{3v} C_9BH_9 (4) and C_s C_8NH_9 (7), respectively.

3.2 Fluxional bonds in $C_9H_9^+$

AdNDP bonding analyses recover both localized and delocalized bonds of the concerned species. As shown in Fig. 2(a), the C_{3v} GS possesses 21 2c-2e σ bonds including 12 C—C σ single bonds and 9 C—H σ single bonds with the occupation numbers of ON = 1.94—1.99 |e| and 1 3c-2e σ bond with ON = 1.96 |e|, among which the 3c-2e σ bond on C3, C4, and C5 at the bottom has been converted into a 2c-2e C3—C4 σ bond in C_{2v} TS. An opposite process occurs from TS → GS′ where the 2c-2e C1—C2 σ bond is converted into a 3c-2e σ bond on C1, C2, and C5 on the top in C_{3v} GS′. Thus, $C_9H_9^+$ undergoes a GS (1 2c-2e σ + 1 3c-2e σ) → TS (2 2c-2e σ) → GS′ (1 2c-2e σ + 1 3c-2e σ) bonding fluctuation which mainly involves two fluxional σ-bonds in a concerted mechanism, as shown in Fig. 2(b). Such a process repeats itself at 950 K in molecular dynamics simulations (Video S1 in the Supporting Information).

3.3 Fluxional bonds in C_9BH_9 and C_8NH_9

As indicated in Fig. 3(a), the bonding fluctuation of C_9BH_9 appears to be similar with that of bullvalene[17]. It mainly involves two fluxional π bonds and one fluxional σ bond in the fluxional process. From C_{3v} GS to C_s

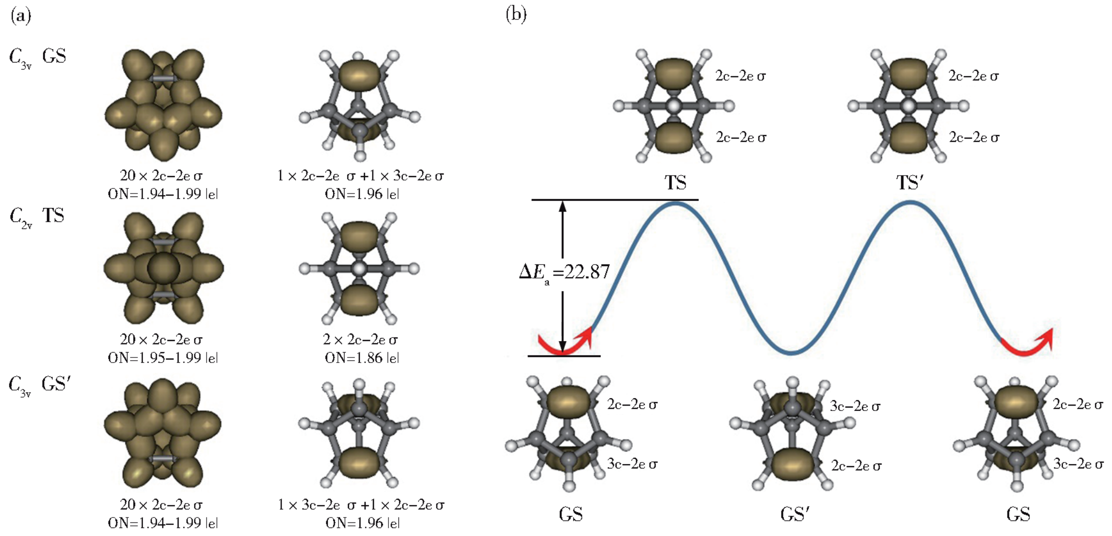

Fig. 2 (a) AdNDP bonding patterns of the GS/GS' and TS of $C_9H_9^+$. (b) σ-bonding fluctuation of $C_9H_9^+$ in the fluxional process of GS→TS→GS'→TS'→GS, with the energy barrier ΔE_a indicated in kcal·mol^{-1}

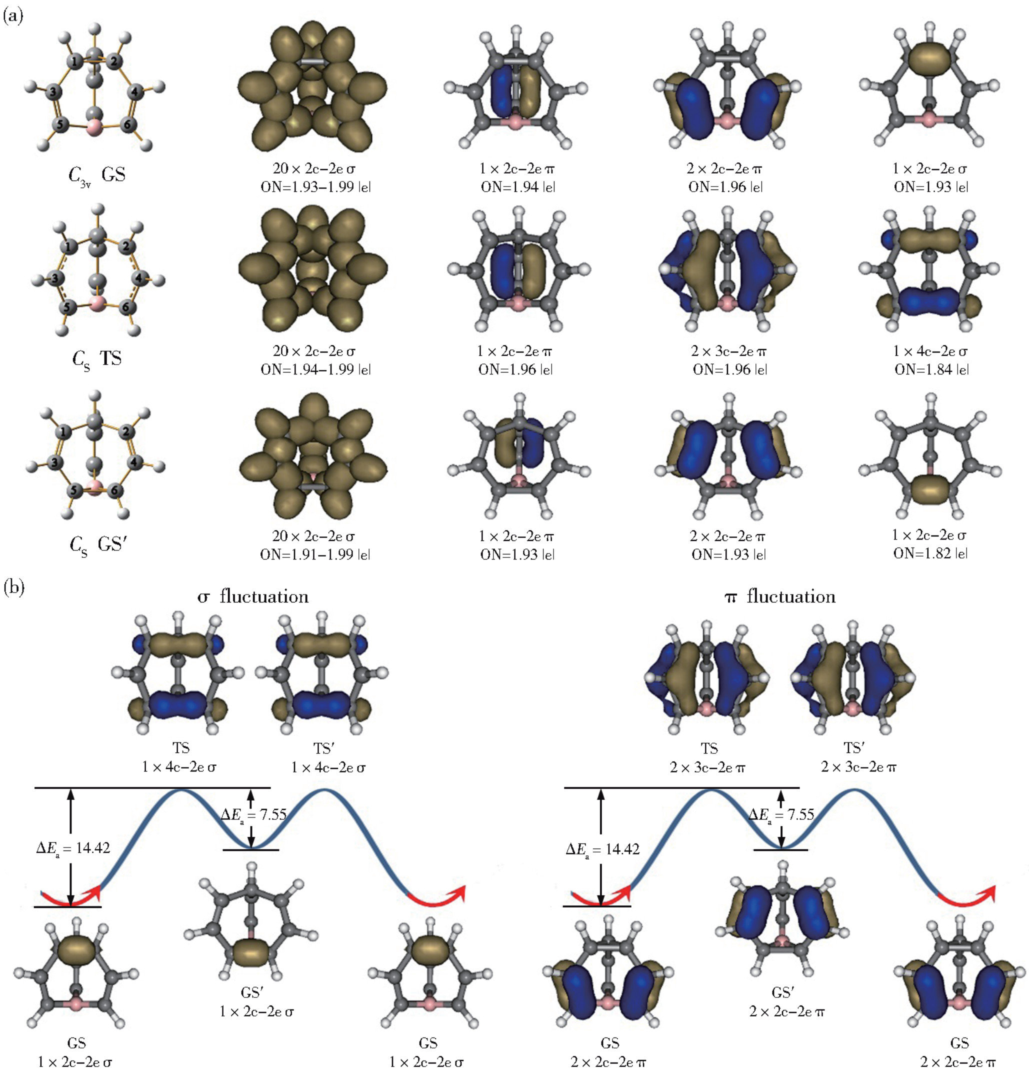

Fig. 3 (a) AdNDP bonding patterns of the GS/GS' and TS of C_9BH_9. (b) σ and π bonding fluctuations of C_9BH_9 in the fluxional process of GS→TS→GS'→TS'→GS, with the energy barrier ΔE_a indicated in kcal·mol^{-1}

Table 1 Calculated standard activation free energies $\Delta G^{\neq}$, transmission coefficient κ, and rate constants k^{TST} of $C_9H_9^+$, C_9BH_9 and C_8NH_9 in the fluxional processes of GS→TS and TS→GS' at the single-point CCSD(T)//PBE0/6-311+G(d) level.

	$C_9H_9^+$		C_9BH_9		C_8NH_9	
	GS→TS	TS→GS′	GS→TS	TS→GS′	GS→TS	TS→GS′
$\Delta G^{\neq}$ / kcal·mol^{-1}	22.76	22.76	14.06	7.69	13.18	7.68
κ	1.288	1.288	1.063	1.063	1.169	1.169
k^{TST} / s^{-1}	1.63×10^{-4}	1.63×10^{-4}	3.22×10^{2}	1.51×10^{7}	1.57×10^{3}	1.69×10^{7}

TS, two 2c-2e π bonds over C3—C5 and C4—C6 are converted into two 3c-2e π bonds over C1⋯C3⋯C5 and C2⋯C4⋯C6 along two edges in the front, while the 2c-2e C1—C2 σ bond on the top is transferred into a 4c-2e σ bond on C1—C2 and C5—C6. The remaining 20 2c-2e σ bonds on the surface and 1 2c-2e π bond at the back are kept basically unchanged in the fluxional process. An opposite process takes place from the C_s TS to C_s GS'. The fluctuation of C_9BH_9 thus involves basically two fluxional π-bonds (GS (2 2c-2e π) → TS (2 3c-2e π) → GS′ (2 2c-2e π)) and one fluxional σ-bond (GS (1 2c-2e σ) → TS (1 4c-2e σ) → GS′ (1 2c-2e σ)) in concerted mechanisms (Fig. 3(b)). We observed this process in molecular dynamics simulations at 800 K (Video S2).

Fig. S1(a) shows the AdNDP bonding pattern of

C_8NH_9 and Fig. S1(b) demonstrates the σ and π bonding fluctuations in it. Similar to $C_{10}H_{10}$ and C_9BH_9, the bonding fluctuation of C_8NH_9 mainly involves two fluxional π-bonds (GS (2 2c-2e π) → TS (2 3c-2e π) → GS′ (2 2c-2e π)) and one fluxional σ-bond (GS (1 2c-2e σ) → TS (1 4c-2e σ) → GS′ (1 2c-2e σ)), while the remaining 19 2c-2e σ bonds remain basically unchanged. The breakage and formation of two π-bonds and one σ-bond of C_8NH_9 occurred at 800 K in molecular dynamics simulations (Video S3). To better visualize the bonding changes in these processes, we simulate the bonding fluctuations of $C_9H_9^+$, C_9BH_9, and C_8NH_9 in Video S4–S6 in the Supporting Information.

4 Summary

We have optimized the GS, TS, and GS′ structures of bullvalene analogs $C_9H_9^+$, C_9BH_9, and C_8NH_9, and analyzed the fluxional bonds in them which facilitate the fluxionality of these cage-like species, unveiling the σ bonding fluxional nature of $C_9H_9^+$ (GS (1 2c-2e σ + 1 3c-2e σ) → TS (2 2c-2e σ) → GS′ (1 2c-2e σ + 1 3c-2e σ)) and σ+π dual bonding fluctuation in both C_9BH_9 and C_8NH_9 (GS (2 2c-2e π) → TS (2 3c-2e π) → GS′ (2 2c-2e π) plus GS (1 2c-2e σ) → TS (1 4c-2e σ) → GS′ (1 2c-2e σ)) in concerted mechanisms. More theoretical and experimental investigations on related fluxional molecules are currently in progresses. Fluxional bonds are expected to exist in various intramolecular rearrangements in organic chemistry and may have important applications in both chemical catalysis and nanomaterials designs.

References:

[1] BERRY R S. Correlation of Rates of Intramolecular Tunneling Processes, with Application to Some Group V Compounds[J]. *J Chem Phys*, 1960, **32**(3): 933-938. DOI: 10. 1063/1. 1730820.

[2] GUTOWSKY H S, HOLM C H. Rate Processes and Nuclear Magnetic Resonance Spectra. II. Hindered Internal Rotation of Amides[J]. *J Chem Phys*, 1956, **25**(6):1228-1234. DOI: 10. 1063/1. 1743184.

[3] CASS M E, HII K K, RZEPA H S. Mechanisms that Interchange Axial and Equatorial Atoms in Fluxional Processes: Illustration of the Berry Pseudorotation, the Turnstile and the Lever Mechanisms via Animation of Transition State Normal Vibrational Modes[J]. *J Chem Educ*, 2006, **83**(2):336. DOI: 10. 1021/ed083p336. 2.

[4] KRAMER G M. CH_5^+ Stability and Mass Spectrometry [J]. *Science*, 1999, **286**(5442): 1051. DOI: 10. 1126/science. 286. 5442. 1051a.

[5] WHITE E T, TANG J, OKA T. CH_5^+: The Infrared Spectrum Observed [J]. *Science*, 1999, **284**(5411): 135-137. DOI: 10. 1126/science. 284. 5411. 135.

[6] MARX D, PARRINELLO M. CH_5^+: The Cheshire Cat Smiles [J]. *Science*, 1999, **284**(5411): 59-61. DOI: 10. 1126/science. 284. 5411. 59.

[7] YAN M, LI H R, ZHAO X Y, *et al.* Fluxional Bonds in Planar B_{19}^-, Tubular Ta@B_{20}^-, and Cage-Like B_{39}^-[J]. *J Comput Chem*. 2019, **40**: 966-970. DOI: 10. 1002/jcc. 25728.

[8] YAN M, LI H R, TIAN X X, *et al.* Fluxional Bonds in Quasi-Planar B_{18}^{2-} and Half-Sandwich MB_{18}^- (M = K, Rb, and Cs) [J]. *J Comput Chem*, 2019, **40**(11): 1227-1232. DOI: 10. 1002/jcc. 25782.

[9] ZHAO X Y, LUO X M, TIAN X X, *et al.* NiB_{10}, NiB_{11}^-, NiB_{12}, and NiB_{13}^+: Half-Sandwich Complexes with the Universal Coordination Bonding Pattern of σ Plus π Double Delocalization[J]. *J Clust Sci*, 2019, **30**(1): 115-121. DOI: 10. 1007/s10876-018-1457-4.

[10] WANG Y J, ZHAO X Y, CHEN Q, *et al.* B_{11}^-: A Moving Subnanoscale Tank Tread[J]. *Nanoscale*. 2015, **7**(38): 16054-16060. DOI: 10. 1039/c5nr03732h.

[11] MARTÍNEZ-GUAJARDO G, SERGEEVA A P, BOLDYREV A I, *et al.* Unravelling Phenomenon of Internal Rotation in B_{13}^+Through Chemical Bonding Analysis [J]. *Chem Commun*, 2011, **47**(22):6242-6244. DOI: 10. 1039/c1cc10821b.

[12] FAGIANI M R, SONG X W, PETKOV P, *et al.* Structure and Fluxionality of B_{13}^+ Probed by Infrared Photodissociation Spectroscopy[J]. *Angew Chem Int Ed*. 2017, **56**(2):501-507. DOI: 10. 1002/anie. 201609766.

[13] WANG Y J, YOU X R, CHEN Q, *et al.* Chemical Bonding and Dynamic Fluxionality of a B_{15}^+ Cluster: A nanoscale Double-Axle Tank Tread [J]. *Phys Chem Chem Phys*, 2016, **18**(23): 15774-15782. DOI: 10. 1039/c6cp02544g.

[14] YANG Y G, JIA D M, WANG Y J, *et al.* A Universal Mechanism of the Planar Boron Rotors B_{11}^-, B_{13}^+, B_{15}^+, and B_{19}^- : Inner Wheels Rotating in Pseudo-Rotating Outer Bearings[J]. *Nanoscale*, 2017, **9**(4): 1443-1448. DOI: 10. 1039/c6nr09074e.

[15] LI H R, ZHANG M, YAN M, *et al.* Fluxional Bonds in

Tubular Molecular Rotors B_3-[Ta@B_{18}] and B_4-[Ta@B_{18}]$^+$ in 18-Electron Configurations[J]. *J Clust Sci*, 2019, **31**(2): 331-336. DOI: 10. 1007/s10876-019-01646-0.

[16] LU X Q, CHEN Q, TIAN X X, *et al*. Predicting Lanthanide Boride Inverse Sandwich Tubular Molecular Rotors with the Smallest Core-Shell Structure[J]. *Nanoscale*, 2019, **11**(44): 21311-21316. DOI: 10. 1039/c9nr07284e.

[17] MA Y Y, YAN M, LI H R, *et al*. Probing the Fluxional Bonding Nature of Rapid Cope Rearrangements in Bullvalene $C_{10}H_{10}$ and Its Analogs C_8H_8, C_9H_{10}, and C_8BH_9[J]. *Sci Rep*, 2019, **9**(1): 17074. DOI: 10. 1038/s41598-019-53488-5.

[18] KOHN W, SHAM L J. Self-Consistent Equations Including Exchange and Correlation Effects[J]. *Phys Rev*, 1965, **140**(4A): 1133-1142. DOI: 10. 1103/PhysRev. 140. A1133.

[19] HOHENBERG P, KOHN W. Inhomogeneous Electron Gas [J]. *Phys Rev*, 1964, **136**:864-871. DOI: 10. 1103/PhysRev. 136. B864.

[20] ADAMO C, BARONE V. Toward Reliable Density Functional Methods Without Adjustable Parameters: The PBE0 Model [J]. *J Chem Phys*, 1999, **110**(13): 6158-6170. DOI: 10. 1063/1. 478522.

[21] KRISHNAN R, BINKLEY J S, SEEGER R, *et al*. Self-Consistent Molecular Orbital Methods. XX. A Basis Set for Correlated Wave Functions[J]. *J Chem Phys*, 1980, **72**(1):650-654. DOI: 10. 1063/1. 438955.

[22] LEE C T, YANG W T, PARR R G. Development of the Colle-Salvetti Correlation-Energy Formula into a Functional of the Electron Density [J]. *Phys Rev B*, 1988, **37**(2):785-789. DOI: 10. 1103/PhysRevB. 37. 785.

[23] FROIDEVAUX V, BORNE M, LABORBE E, *et al*. Study of the Diels-Alder and Retro-Diels-Alder Reaction between Furan Derivatives and Maleimide for the Creation of New Materials [J]. *RSC Advances*, 2015, **5**(47):37742-37754. DOI: 10. 1039/C5RA01185J.

[24] FRISCH M J, TRUCKS G W, SCHLEGEL H B, *et al*. Gaussian 09, Revision D. 01[CP]. Gaussian, Inc, Wallingford, CT, 2009.

[25] PURVIS G D, BARTLETT R J. A Full Coupled-Cluster Singles and Doubles Model: The Inclusion of Disconnected Triples[J]. *J Chem Phys*, 1982, **76**(4): 1910-1918. DOI: 10. 1063/1. 443164.

[26] ČÍŽEK J, LEFEBVRE R, MOSER C. On the Use of the Cluster Expansion and the Technique of Diagrams in Calculations of Correlation Effects in Atoms and Molecules[J]. *Adv chem Phys*, 1969, **14**: 35-89. DOI: 10. 1002/9780470143599. ch2.

[27] RAGHAVACHARI K, TRUCKS G W, POPLE J A, *et al*. A Fifth-Order Perturbation Comparison of Electron Correlation Theories [J]. *Chem Phys Lett*, 1989, **157**(6): 479-483. DOI: 10. 1016/S0009-2614(89)87395-6.

[28] WERNER H J, KNOWLES P J, KNIZIA G, *et al*. Molpro: A General-Purpose Quantum Chemistry Program Package[J]. *WIREs: Comput Mol Sci*, 2012, **2**(2): 242-253. DOI: 10. 1002/wcms. 82.

[29] ZUBAREV D Y, BOLDYREV A I. Developing Paradigms of Chemical Bonding: Adaptive Natural Density Partitioning[J]. *Phys Chem Chem Phys*, 2008, **10**(34): 5207-5217. DOI: 10. 1039/b804083d.

[30] ZUBAREV D Y, BOLDYREV A I. Revealing Intuitively Assessable Chemical Bonding Patterns in Organic Aromatic Molecules *via* Adaptive Natural Density Partitioning[J]. *J Org Chem*, 2008, **73**(23): 9251-9258. DOI: 10. 1021/jo801407e.

[31] EYRING H. The Activated Complex in Chemical Reactions[J]. *J Chem Phys*, 1935, **3**(2):107-115. DOI: 10. 1063/1. 1749604.

[32] LAIDLER K J, KING M C. The Development of Transition-State Theory[J]. *J Phys Chem*, 1983, **87**(15): 2657-2664. DOI: 10. 1021/j100238a002.

[33] WIGNER E. Über das Überschreiten von Potentialschwellen Bei Chemischen Reaktionen[J]. *Z Phys Chem*. 1932, **19**:203-216. DOI: 10. 1007/978-3-642-59033-7_8.